ORIGINAL ARTICLE

Initial clinical experience of a prototype ultra-high-resolution CT for assessment of small intracranial arteries

Hiroyuki Nagata[1] · Kazuhiro Murayama[1] · Shigetaka Suzuki[1] · Ayumi Watanabe[1] · Motoharu Hayakawa[2] ·
Yasuo Saito[3] · Kazuhiro Katada[4] · Hiroshi Toyama[1]

Abstract

Purpose Diagnostic and neurosurgical procedures require the precise localization of small intracranial arteries, but this may be difficult using conventional computed tomography angiography (CTA). This study was conducted to evaluate the quality of CTA images acquired using a prototype ultra-high-resolution computed tomography (U-HRCT) system compared with those acquired using a conventional computed tomography (C-CT) system.

Materials and methods From July through September 2015, 10 adult patients (6 women and 4 men) previously scanned by C-CT were examined using U-HRCT to locate and assess cerebral aneurysms. The bilateral ophthalmic artery (Opth A), anterior choroidal artery (Acho A), and thalamoperforating arteries (TPAs) were visually evaluated in randomly presented CTA images. Images were graded on a 5-point scale, and differences in scores between U-HRCT and C-CT were evaluated by the Wilcoxon signed-rank test. A p value < 0.05 was considered statistically significant.

Results Visual evaluation scores for images of the Opth A, Acho A, and TPAs were significantly higher for U-HRCT than for C-CT. U-HRCT images achieved good visualization (score > 3) for C-CT images with poor visualization (score < 3) in 66.7–100% of all the small arteries.

Conclusion U-HRCT is superior to C-CT for detecting and evaluating clinically significant small intracranial arteries.

Keywords Ultra-high-resolution computed tomography · Small intracranial arteries · Computed tomography angiography

Introduction

Small intracranial arteries are frequently involved in cerebral disorders [1–5]. However, these small arteries are often difficult to visualize using conventional neuroimaging modalities. Before surgical intervention to repair a cerebral aneurysm, it is important to precisely determine the positional relationships between the aneurysm and clinically important small arteries such as the thalamoperforating arteries (TPAs), ophthalmic artery (Opth A), and anterior choroidal artery (Acho A). However, visualizing small intracranial arteries by CT angiography (CTA) using conventional CT (C-CT) is difficult due to the partial volume effect associated with the relatively large detector element size (0.5×0.5 mm). Recent advances in CT technology include improved multi-row detector performance in multi-slice CT (MSCT) and area detector CT (ADCT), which facilitate high-speed and wide field-of-view (FOV) imaging as well as functional evaluation. However, the in-plane spatial resolution, which is one of the essential performance criteria for CT imaging, is not substantially increased in C-CT. The ultra-high-resolution CT (U-HRCT) system which has been newly developed by the National Cancer Center and Canon Medical Systems Corporation employs detector elements measuring 0.25×0.25 mm, which is one-fourth the area of the elements in a conventional CT

✉ Hiroyuki Nagata
nagata_zaiken@yahoo.co.jp

1 Department of Radiology, Fujita Health University, 1-98 Dengakugakubo, Kutsukake-cho, Toyoake, Aichi 470-1101, Japan

2 Department of Neurosurgery, Fujita Health University, 1-98 Dengakugakubo, Kutsukake-cho, Toyoake, Aichi 470-1101, Japan

3 CT Systems Division, Canon Medical Systems Corporation, 1385 Shimoishigami, Otawara-shi, Tochigi 324-0036, Japan

4 Joint Research Laboratory of Advanced Medical Imaging, Fujita Health University, 1-98 Dengakugakubo, Kutsukake-cho, Toyoake, Aichi 470-1101, Japan

detector. In 2005, 4-row U-HRCT was applied clinically for the first time, and in 2015, 128-row U-HRCT(TSX-304R) was developed, providing even higher resolution in clinical imaging. Kakinuma et al. [6] demonstrated that 4-row U-HRCT can enhance the spatial resolution of images of lung lesions. In previous studies, Zhu et al. [7] and Sheshadri et al. [8] reported that using a small scan FOV improved image quality compared to C-CT, particularly with regard to airway dimensions and subsolid nodules in a limited area. Hata et al. [9] reported that a large matrix size in U-HRCT improved image quality and the assessment of lung diseases. Yoshioka et al. [10] reported that U-HRCT was superior to C-CT for visual evaluation of the artery of Adamkiewicz in patients with thoracic and thoraco-abdominal aneurysms.

While smaller detector elements enhance the spatial resolution of CT images by reducing the partial volume effect, the performance of U-HRCT for the visualization of small intracranial arteries has not been evaluated. In the present study, visual evaluation scores of U-HRCT and C-CT images were directly compared to determine whether the higher resolution of U-HRCT can improve diagnostic performance.

Materials and methods

Subjects

This study received the approval of the institutional review board of our hospital. Our institutional review board approved this opt-out research design. Opt-out opportunities were provided to all the participants included in this retrospective study. The prototype U-HRCT in this study is a medical device that has obtained the certification as a CT scanner on April 7, 2015 (Identification number: 227ADBZX00062000) and has no problem regarding clinical use.

From July through September 2015, total 12 consecutive patients (11 patients with cerebral aneurysm and 1 patient with cerebral artery stenosis) examined using a 320-row C-CT system (Aquilion ONE/VISION; Canon Medical Systems, Otawara, Japan) for cerebral aneurysms or cerebral artery stenosis were re-examined using a prototype U-HRCT system (TSX-304R; Canon Medical Systems) prior to surgery or during follow-up. Of these 12 patients, 10 (6 women and 4 men; age range 52–83 years; mean age 69.0 years) were enrolled in the study after 2 patients (1 patient with cerebral aneurysm and 1 patient with cerebral artery stenosis) were excluded due to body movement or unsatisfactory equipment settings in CTA acquisition. Time interval between CTA scans of C-CT and U-HRCT was 174–484 days (mean 322.2 days) (Table 1). The size and shape of all the aneurysms were not changed during this interval.

Table 1 Clinical characteristics of 10 patients

Characteristics	Values
Age, years	Mean: 69.0, range: 52–83
Gender	6 women, 4 men
Location of cerebral aneurysms	
Internal carotid artery	5
Middle cerebral artery	3
Anterior cerebral artery	2
Anterior communicating artery	1
Basilar artery	1
Basilar artery—superior cerebellar artery	1
Time interval between CTA scans of C-CT and U-HRCT, days	Mean: 322.2, range: 174–484

C-CT conventional CT, *U-HRCT* ultra-high-resolution CT

CTA protocol and post-processing

The U-HRCT scanner used in this study is equipped with a 128-row detector. The detector matrix is 1792 channels × 128 rows, and each detector element is 0.25 mm × 0.25 mm at the isocenter. The beam collimation is 0.25 mm × 128 or 32 mm at the isocenter. The small focal spot of the X-ray tube is 0.6 mm × 0.6 mm and the maximum output with the small focus is 120 kV and 290 mA or 135 kV and 260 mA.

The image acquisition conditions for U-HRCT were as follows: slice thickness 0.25 mm × 128-row helical scan, tube voltage 135 kV, tube current set by automatic tube current setting, standard deviation 5.70, rotation time 1 s, beam pitch 0.625, and 1024 × 1024 matrix image reconstruction. The imaging conditions for C-CT were as follows: slice thickness 0.5 mm × 20-row non-helical scan, tube voltage 120 kV, tube current set by automatic tube current setting, standard deviation 4.00, rotation time 1 s, 512 × 512 matrix image reconstruction. Prior to CTA, iopamidol contrast medium (Iopamiron 370; Bayer, Osaka, Japan) was injected at an equivalent dose of 370 mg iodine per milliliter (mgI/mL) at a rate of 25.0 mgI/kg/s for 10 s, followed by a 30 mL saline flush injected at the same rate using a dual-head injector. Established venous access was due to use of right basilica vein according to scanning protocol. CTA scanning started using manual bolus tracking technique applied in the internal carotid artery at the foramen magnum level.

In this study, the acquired images were reconstructed using a successive approximation application reconstruction method known as Adaptive Iterative Dose Reduction 3D (AIDR 3D; Canon Medical Systems) [11–14]. In addition to planar scans, axial U-HRCT images were

reconstructed with a slice thickness of 0.25 mm, and 5-mm maximum intensity projection (MIP) images were also generated from the reconstructed data. All the observers were not involved in image reconstruction.

Data analysis

The small intracranial arteries which were the target for evaluation in this study were the bilateral Opth A, bilateral

Acho A, and TPAs. Opth A and Acho A on both sides were evaluated, respectively. Two corresponding images obtained using U-HRCT and C-CT were randomly presented to two board-certified radiologists (K.M. and S.S., both with 14 years of experience) and two resident radiologists (A.W. and H.N., both with 5 years of experience) who performed visual evaluation using a 5-point grading system based on the shape of the bifurcation and the continuity and visibility of the small intracranial arteries as they extended toward the image periphery. All the observers did not know any

Fig. 1 The reference images of anterior choroidal artery reconstructed by 5-mm sagittal MIP (Acho A, bifurcation and continuity, white arrow). **a** 1 point of Acho A bifurcation. **b** 3 point of Acho A bifurcation. **c** 5 point of Acho A bifurcation. **d** 1 point of Acho A continuity. **e** 3 point of Acho A continuity. **f** 5 point of Acho A continuity
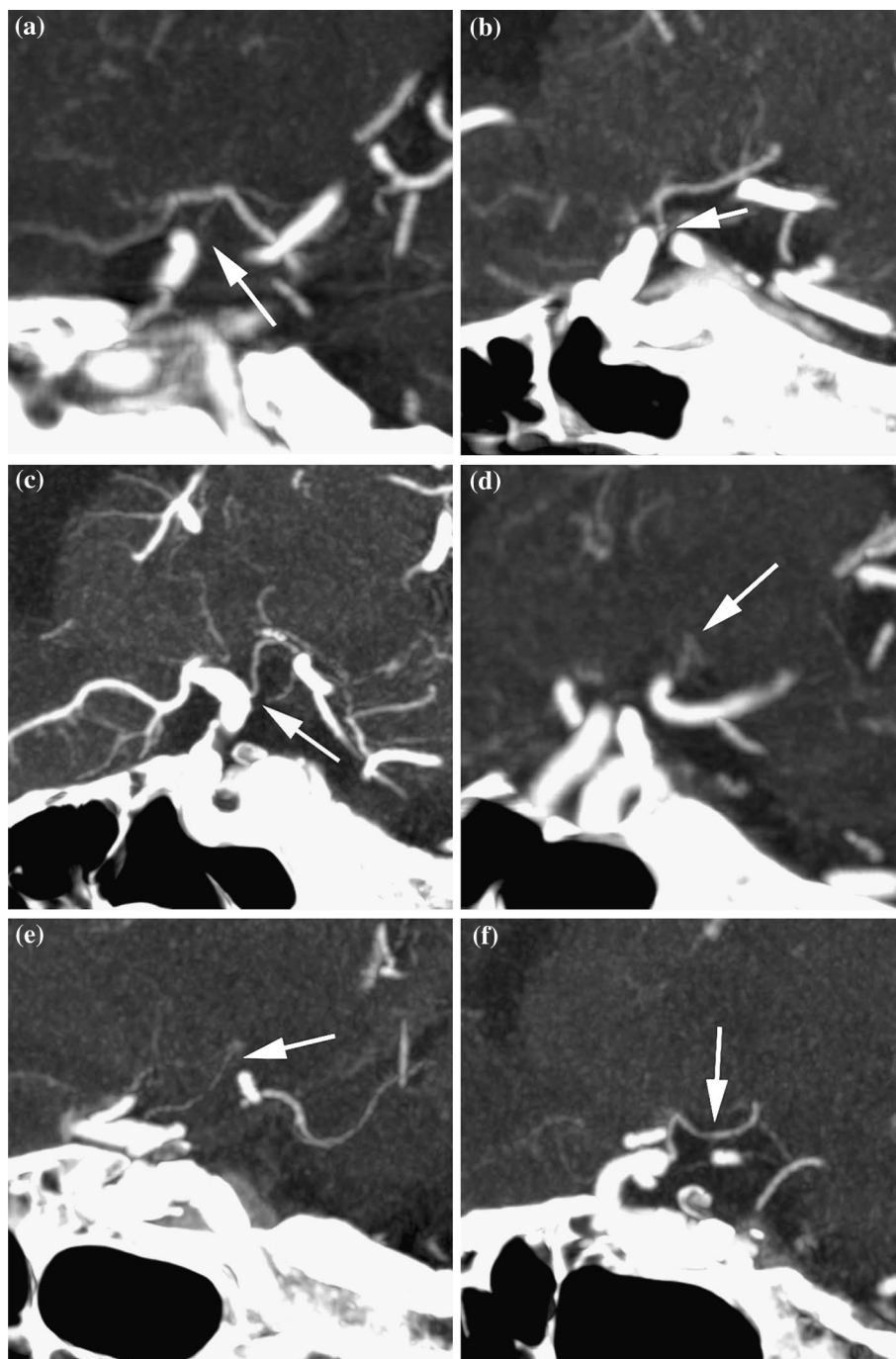
Fig. 2 Visual evaluation scores for ultra-high-resolution CT (U-HRCT) and conventional CT (C-CT) images of the ophthalmic artery (Opth A) (**a** bifurcation, **b** continuity), anterior choroidal artery (Acho A) (**c** bifurcation, **d** continuity), and thalamoperforating arteries (TPAs) (**e** bifurcation). The visual evaluation scores of all small intracranial arteries are significantly higher for U-HRCT images than for C-CT images (*$p < 0.05$)
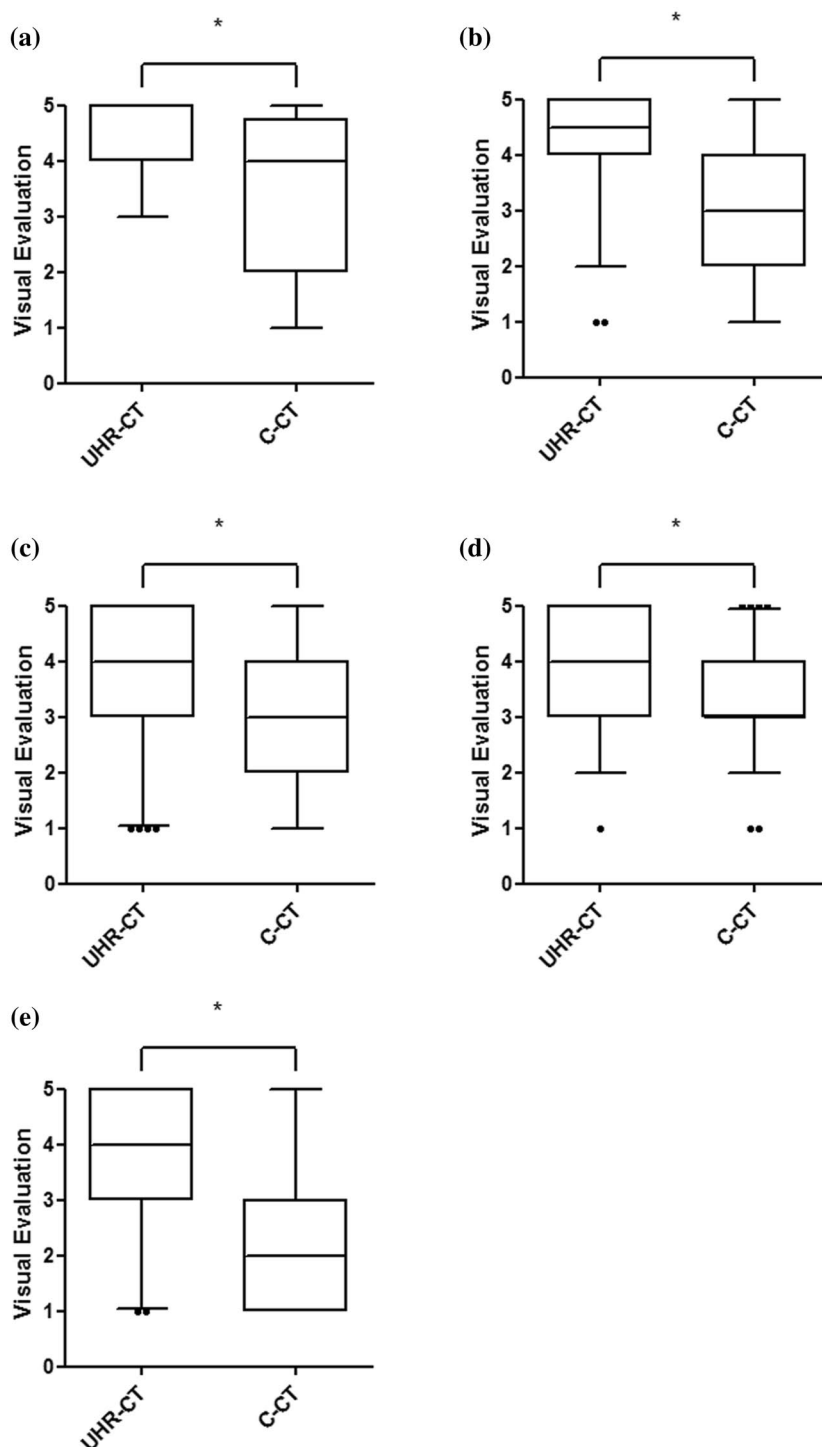
information about the images when they evaluated the CTA images. Specifically, evaluation was performed individually in the following order from (1) to (5): (1) shape of the bilateral Opth A bifurcation, (2) continuity of the bilateral Opth A, (3) shape of the bilateral Acho A bifurcation, (4) peripheral continuity of the bilateral Acho A, and (5) shape of the TPA bifurcation. Since only one TPA was detected

on CTA in some cases, the bilateral TPAs for two arteries were evaluated as one judgment using the best grade score. The grading system for image evaluation was as follows: 1 point, identification of continuity of the blood vessel to the bifurcation or periphery is difficult; 2 points, only a shadow suggestive of continuity of the blood vessel to the bifurcation or periphery is observed; 3 points, continuity of the
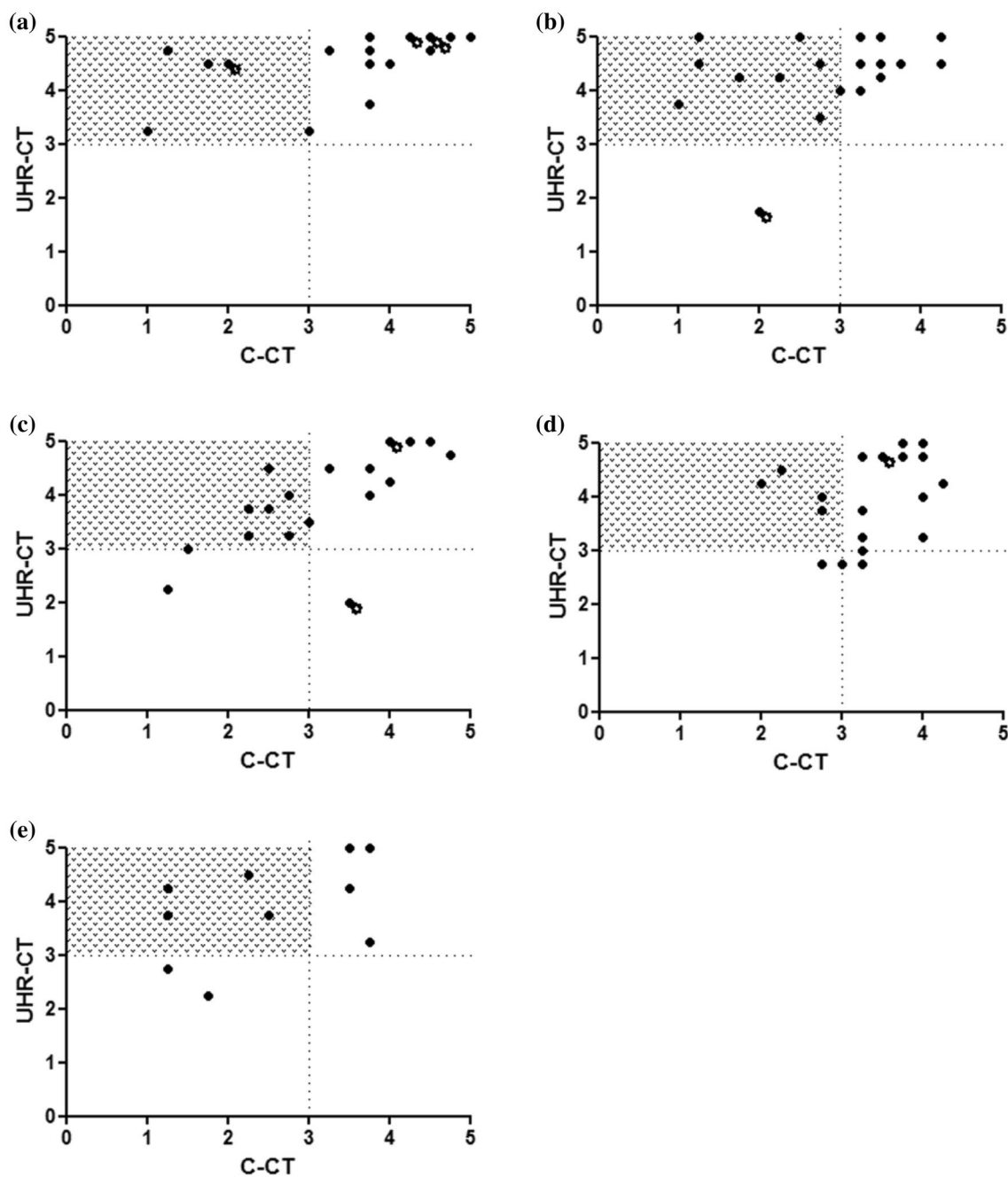
Fig. 3 Relationships between ultra-high-resolution CT (U-HRCT) and conventional CT (C-CT) scores of the ophthalmic artery (Opth A) (**a** bifurcation, **b** continuity), anterior choroidal artery (Acho A) (**c** bifurcation, **d** continuity), and thalamoperforating arteries (TPAs) (**e** bifurcation) in each artery. The black circles indicate the visual evalu-ation scores for each artery. The overlapped same scores are plotted adjacent to the lower right (closed circles). The shaded areas indicate good visualization (score > 3) for U-HRCT images and poor visuali-zation (score < 3) for C-CT images

blood vessel to the bifurcation or periphery can be roughly determined; 4 points, continuity of the blood vessel to the bifurcation or periphery can be identified along most of its course; and 5 points, continuity of the blood vessel to the bifurcation or periphery is clearly visualized. Figure 1 shows the reference images of Acho A bifurcation and continuity.

All the observers conducted a preliminary estimation using another CTA images before this study. A score > 3 was con-sidered good visualization, and a score < 3 was considered poor visualization. The Opth A bifurcation was viewed in axial tomographic images. In addition, the peripheral course and bifurcation of the Opth A and the peripheral course of

Fig. 4 CTA images of a patient with a basilar artery tip aneurysm. **a** 5-mm coronal MIP image acquired using C-CT. Only the left thalamoperforating artery (TPA) (white arrow) originating from the proximal left posterior cerebral artery is seen. **b** 5-mm coronal MIP image acquired using U-HRCT. Both the right (white arrowhead) and left (white arrow) TPAs are seen. **c** 5-mm axial MIP image acquired using C-CT. Only the left TPA (white arrow) is seen. **d** 5-mm axial MIP image acquired using U-HRCT. Both the right (white arrowhead) and left (white arrow) TPAs are seen
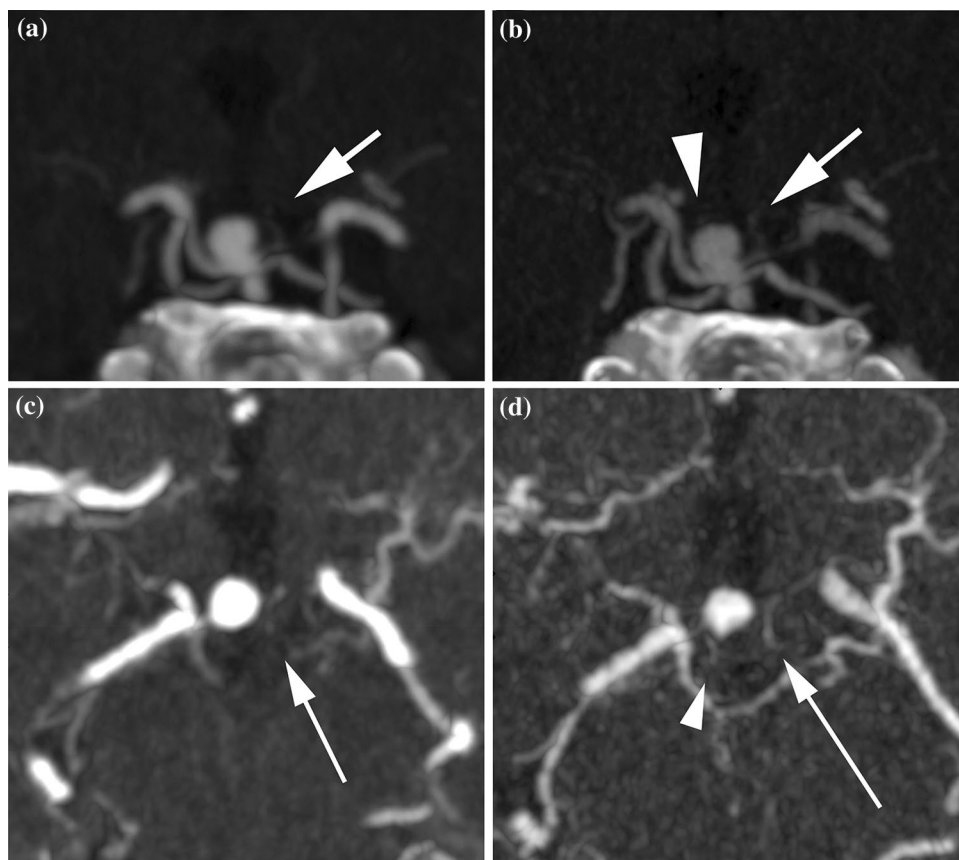
the Acho A were viewed in sagittal tomographic images with 5-mm MIP. The TPAs were viewed in coronal tomographic images with 5-mm MIP. A 1024×1024 pixel monitor (Radi-Forse RS110; EIZO Corporation, Shinagawa, Japan) was used for evaluation of both U-HRCT and C-CT images. The scatter plots for average visual evaluation scores of U-HRCT were compared with those of C-CT, respectively.

Radiation dose

The radiation dose was evaluated using the volume CT dose index ($CTDI_{vol}$) and the dose length product (DLP), both of which were displayed on the CT console in each examination. The radiation dose was also compared against the diagnostic reference level (DRL) of the Japan Network for Research and Information on Medical Exposure (J-RIME).

Statistical analysis

The visual evaluation scores for all five items were compared using the Wilcoxon signed-rank test. GraphPad Prism (Version 5; GraphPad Software, San Diego, CA) was used for statistical analysis. A p value < 0.05 was considered statistically significant.

We assessed interobserver agreement between board-certified radiologists and resident radiologists for average visual evaluation scores performed U-HRCT by Kappa statistics. The Kappa values were interpreted as follows: 0–0.20 was weak, 0.21–0.40 was fair, 0.41–0.60 was moderate, 0.61–0.80 was good, and 0.81–1.00 was excellent; the higher Kappa values, the stronger is the agreement between the board-certified radiologists and resident radiologists.

Results

Based on the 5-point grading system employed in this study, the visual evaluation scores of all the small intracranial arteries evaluated were significantly higher for U-HRCT images than for C-CT images as follows: Opth A: 4.6 ± 0.7 vs. 3.5 ± 1.3 (bifurcation), Opth A: 4.2 ± 1.1 vs. 2.8 ± 1.3 (continuity), Acho A: 3.9 ± 1.2 vs. 3.2 ± 1.3 (bifurcation), Acho A: 4.0 ± 1.0 vs. 3.3 ± 0.9 (continuity), and TPAs: 3.9 ± 1.2 vs. 2.5 ± 1.3 (bifurcation) (Fig. 2). U-HRCT images achieved good visualization (score > 3) for C-CT images with poor visualization (score < 3) as follows: 6 of 6 arteries (100%) for the Opth A (bifurcation), 9 of 11 arteries (81.8%) for the Opth A (continuity), 7 of 9 arteries (77.7%)
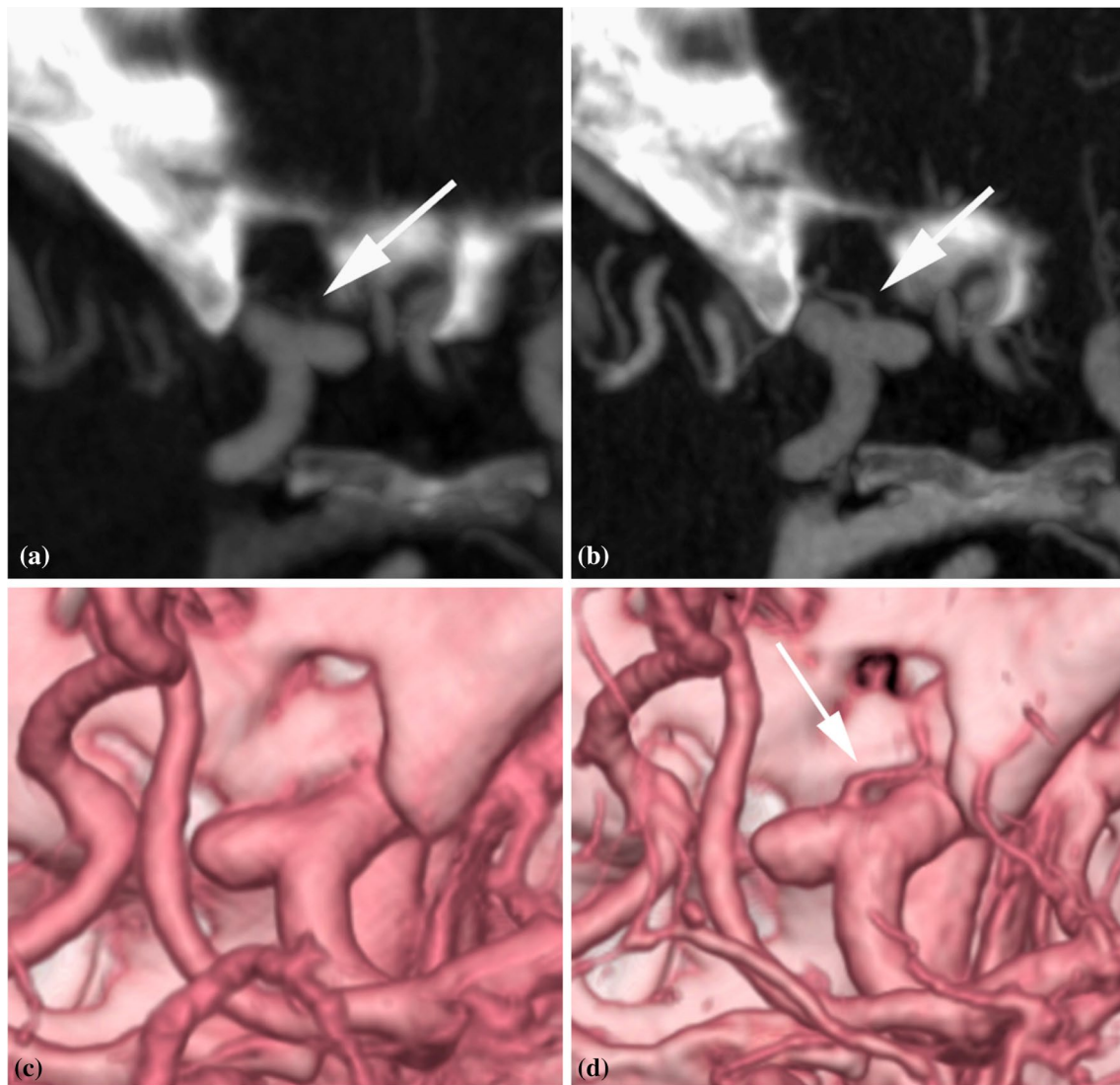
Fig. 5 Images of a patient with a right internal carotid artery aneurysm. **a** 5-mm axial MIP image acquired using C-CT. It is difficult to see the right ophthalmic artery (Opth A) (white arrow). **b** 5-mm axial MIP image obtained using U-HRCT. The right Opth A (white arrow) is clearly seen. **c** Volume-rendered image generated from C-CT data. The right Opth A is not seen. **d** Volume-rendered image generated from U-HRCT data. The right Opth A (white arrow) is clearly seen

for the Acho A (bifurcation), 4 of 6 arteries (66.7%) for the Acho A (continuity), and 4 of 6 arteries (66.7%) for the TPAs (bifurcation) (Fig. 3). The CTA images obtained by U-HRCT were clearer than those obtained using C-CT for all visual evaluation items (Figs. 4, 5, 6).The interobserver coefficients for U-HRCT (0.7515) and C-CT (0.7630) indicated good agreement.

Radiation dose

Both the mean $CTDI_{vol}$ and DLP were significantly higher for U-HRCT acquisition than C-CT acquisition ($CTDI_{vol}$: 75.49 ± 8.89 mGy vs. 48.36 ± 9.25 mGy; DLP: 868.8 ± 114.5 mGy cm vs. 386.9 ± 73.9 mGy cm). However, the radiation doses for U-HRCT were still lower than the DRL according to J-RIME (85 mGy and 1350 mGy cm) (Table 2).

Discussion

The intracranial CTA images obtained using a prototype U-HRCT system with 0.25×0.25 mm detector elements were superior to those obtained using a C-CT system with regard to visualization of Opth A and Acho A bifurcation and peripheral continuity and TPA bifurcation. Our U-HRCT system is equipped with detector elements that are one-fourth the area of the detector elements in a C-CT system, conferring higher spatial resolution and reduced partial volume effect.

Small intracranial arteries may be a source of severe complications in many central nervous system disorders [15, 16]. In patients with aneurysms, it is crucial to evaluate the spatial relationships with surrounding small intracranial arteries, but these small arteries are not always visible in C-CT images due to the limited spatial resolution. Since the visualization of small intracranial arteries is improved in U-HRCT, more precise evaluation is possible compared to C-CT. However, 3 arteries showed that the C-CT images were superior to the U-HRCT images on Acho A. We considered that artifact of posterior clinoid process affected the improvement in the image quality adversely.

The TPAs are often too thin to be visualized using C-CT, necessitating the use of digital subtraction angiography (DSA) [17–19]. In the present study, U-HRCT achieved good visualization in 67% of the C-CT images with poor visualizat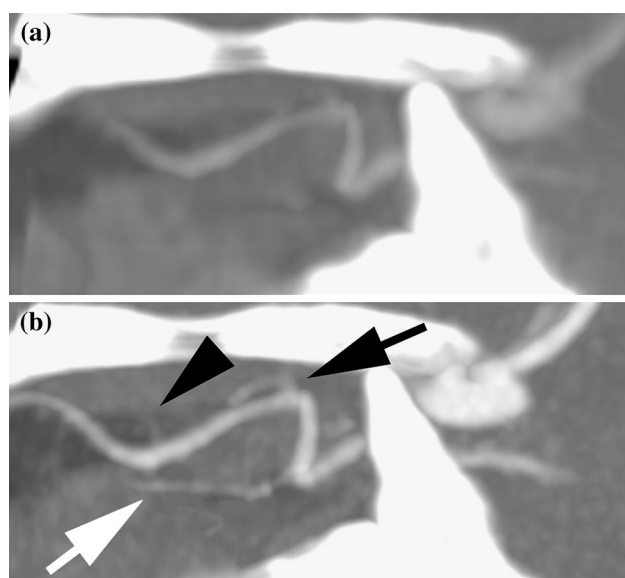ion. Since clinically important small arteries such as the TPAs can be visualized in CTA images acquired using U-HRCT, these small intracranial arteries can now be evaluated non-invasively [20–22]. However, if the diameter of the small arteries is equal to or smaller than the detector element size, visualization may be challenging even with U-HRCT.

Since the interobserver agreement by Kappa statistics were good for U-HRCT systems, U-HRCT was effective in evaluating the smaller intracranial arteries for resident radiologists.

A 4-fold increase in radiation dose is needed theoretically for the U-HRCT scanning because U-HRCT employs detector elements that are one-fourth the area of those used in a conventional CT detector. In the present study, the radiation dose in U-HRCT was approximately twice as high as the radiation dose of C-CT. Since sufficient radiation dose is applied to the patient in the C-CT examination, the spatial resolution of C-CT may be hardly changed even if the radiation dose of the C-CT is increased to the same as that of U-HRCT. Despite the lower radiation dose, excellent CTA visualization was still achieved, which is attributable to the greater impact of the smaller detector element size and the concomitant reduction in the partial volume effect. Further technical advances in noise reduction techniques are anticipated in the near future.

This study has several limitations. First, the U-HRCT system used was a prototype, and the number of subjects was small during the limited period of the study. Second, C-CT with an area detector performs intracranial CTA acquisition in a single rotation, whereas U-HRCT requires the use of helical scanning, in which the longer scanning time leads to a greater possibility of motion artifacts and variations in contrast enhancement. Third, only three kinds of arteries (Opth A, Acho A and TPAs) which are known as representative arteries in predilection areas of intracranial aneurysms were evaluated in this initial clinical study. However, further studies would be required to evaluate other important small arteries, including lenticulostriate artery and recurrent artery of Heubner.

In conclusion, intracranial CTA using U-HRCT was found to be superior to C-CT for the visual evaluation of small intracranial arteries (Opth A, Acho A and TPAs). Head CTA using U-HRCT may allow the clear visualization of small intracranial arteries that are difficult to detect by C-CT.

Fig. 6 Images of the intraorbital ophthalmic artery. **a** 5-mm sagittal MIP image acquired using C-CT. The main ophthalmic artery (Opth A) is seen, but its branches are not. **b** 5-mm sagittal MIP image acquired using U-HRCT. The lacrimal artery (black arrow), anterior ethmoidal artery (black arrowhead), and retinal artery (white arrow) are seen

Table 2 Comparison of radiation doses for U-HRCT and C-CT imaging

Group	C-CT (Mean ± SD)	U-HRCT (Mean ± SD)	DRL (J-RIME)
$CTDI_{vol}$ (mGy)	48.36 ± 9.247	75.49 ± 8.886	85
DLP (mGy cm)	386.9 ± 73.94	868.8 ± 114.5	1350

C-CT conventional CT, *U-HRCT* ultra-high-resolution CT, *DRL* diagnostic reference level, *J-RIME* Japan Network for Research and information on Medical Exposure, *SD* standard deviation, *CTDIvol* volumetric computed tomography dose index, DLP dose length product

Compliance with ethical standards

Ethical statement This article does not contain any studies with human participants or animals performed by any of the authors. This study received the approval of the institutional review board of our hospital.

References

1. Rhoton AL Jr, Fujii K, Fradd B. Microsurgical anatomy of the anterior choroidal artery. Surg Neurol. 1979;12(2):171–87.
2. Rosner SS, Rhoton AL Jr, Ono M, Barry M. Microsurgical anatomy of the anterior perforating arteries. J Neurosurg. 1984;61:468–85.
3. Segarra JM. Cerebral vascular disease and behavior. I. The syndrome of the mesencephalic artery (basilar artery bifurcation). Arch Neurol. 1970;22:408–18.
4. Castaigne P, Lhermitte F, Buge A, Escourolle R, Hauw JJ, Lyon-Caen O. Paramedian thalamic and mid brain infarct: clinical and neuropathological study. Ann Neurol. 1981;10:127–48.
5. Lazzaro NA, Wright B, Castillo M, Fischbein NJ, Glastonbury CM, et al. Artery of percheron infarction: imaging patterns and clinical spectrum. AJNR Am J Neuroradiol. 2010;31:1283–9.
6. Kakinuma R, Moriyama N, Muramatsu Y, Gomi S, Suzuki M, Nagasawa H, et al. Ultra-high-resolution computed tomography of the lung: image quality of a prototype scanner. PLoS ONE. 2015;10:e0137165.
7. Zhu H, Zhang L, Wang Y, Hamal P, You X, Mao H, et al. Improved image quality and diagnostic potential using ultra-high-resolution computed tomography of the lung with small scan FOV: a prospective study. PLoS ONE. 2017;12:e0172688.
8. Sheshadri A, Rodriguez A, Chen R, Kozlowski J, Burgdorf D, Koch T, et al. Effect of reducing field of view on multidetector quantitative computed tomography parameters of airway wall thickness in asthma. J Comput Assist Tomogr. 2015;39:584–90.
9. Hata A, Yanagawa M, Honda O, Kikuchi N, Miyata T, Tsukagoshi S, et al. Effect of matrix size on the image quality of ultra-high-resolution CT of the lung: comparison of 512×512, 1024×1024, and 2048×2048. Acad Radiol. 2018;25:869–76.
10. Yoshioka K, Tanaka R, Takagi H, Ueyama Y, Kikuchi K, Chiba T, et al. Ultra-high-resolution CT angiography of the artery of Adamkiewicz: a feasibility study. Neuroradiology. 2018;60:109–15.
11. Matsuki M, Murakami T, Juri H, Yoshikawa S, Narumi Y. Impact of adaptive iterative dose reduction (AIDR) 3D on low-dose abdominal CT: comparison with routine-dose CT using filtered back projection. Acta Radiol. 2013;54:869–75.
12. Moscariello A, Takx RA, Schoepf UJ, Renker M, Zwerner PL, O'Brien TX, et al. CoronaryCT angiography: image quality, diagnostic accuracy, and potential for radiation dose reduction using a novel iterative image reconstruction technique-comparison with traditional filtered back projection. EurRadiol. 2011;21:2130–8.
13. Singh S, Kalra MK, Gilman MD, Hsieh J, Pien HH, Digumarthy SR, et al. Adaptivestatisticaliterativereconstructiontechnique for radiation dose reduction in chest CT: a pilot study. Radiology. 2011;259:565–73.
14. Kalra MK, Woisetschläger M, Dahlström N, Singh S, Lindblom M, Choy G, et al. Radiationdosereduction with Sinogram Affirmed Iterative Reconstruction technique for abdominal computed tomography. J Comput Assist Tomogr. 2012;36(3):339–46.
15. Brinjikji W, Murad MH, Lanzino G, Cloft HJ, Kallmes DF. Endovascular treatment of intracranial aneurysms with flow diverters: a meta-analysis. Stroke. 2013;44:442–7.
16. Heiskanen O. Risks of surgery for unruptured intracranial aneurysms. J Neurosurg. 1986;65:451–3.
17. Cao W, Dong Q, Li L, Dong Y. Bilateral thalamic infarction and DSA demonstrated AOP after thrombosis. Acta Radiol Short Rep. 2012. https://doi.org/10.1258/arsr.2012.110004.
18. Griessenauer CJ, Loukas M, Tubbs RS, Cohen-Gadol AA. The artery of Percheron: an anatomic study with potential neurosurgical and neuroendovascular importance. Br J Neurosurg. 2014;28:81–5.
19. Kocaeli H, Yilmazlar S, Kuytu T, Korfalı E. The artery of Percheron revisited: a cadaveric anatomical study. Acta Neurochir (Wien). 2013;155:533–9.
20. Marinković S, Gibo H, Brigante L, Nikodijević I, Petrović P. The surgical anatomy of the perforating branches of the anterior choroidal artery. Surg Neurol. 1999;52(1):30–6.
21. Saeki N, Rhoton AL Jr. Microsurgical anatomy of the upper basilar artery and the posterior circle of Willis. J Neurosurg. 1977;46(5):563–78.
22. Kim SH, Yeo DK, Shim JJ, Yoon SM, Chang JC, Bae HG. Morphometric study of the anterior thalamoperforating arteries. J Korean Neurosurg Soc. 2015;57(5):350–8.